Acta Crystallographica Section D
Biological Crystallography
ISSN 0907-4449

Structural studies on the binding of 4-methylumbelliferone glycosides of chitin to rainbow trout lysozyme

Valentina Burkow Vollan, Edward Hough and Solveig Karlsen*

Protein Crystallography Group, Department of Chemistry, Faculty of Science, University of Tromsø, N-9037 Tromsø, Norway

Correspondence e-mail: solveig.karlsen@chem.uit.no

Received 13 March 1998
Accepted 6 May 1998

PDB References: lysozyme–4-methylumbelliferyl chitobioside, 1bb6; lysozyme–4-methylumbelliferyl chitobioside, 1bb7.

Two complexes between rainbow trout lysozyme (RBTL) and 4-methylumbelliferyl chitobioside, 4MeU-$(GlcNAc)_2$, and chitotrioside, 4MeU-$(GlcNAc)_3$, were produced by co-crystallization and soaking, respectively, and the crystal structures were solved at 2.0 Å resolution. The results show that 4-MeU-$(GlcNAc)_3$ binds in subsites *A*–*D* and that 4-MeU-$(GlcNAc)_2$ binds in subsites *B*–*D* in the active-site cleft of RBTL. This agrees well with earlier crystallographic studies on the binding of oligosaccharides of chitin to RBTL, which showed that $(GlcNAc)_3$ binds to sites *B*–*D* in RBTL and not to *A*–*C* as seen in the human and turkey egg-white lysozymes. For both complexes the 4-MeU moiety in site *D* has diffuse electron density and is flexible, as it is only bound to water molecules and not to the protein. Since no electron density was observed in site *E*, the solved structures give views of nonproductive enzyme–substrate complexes.

1. Introduction

In addition to being 1,4-β-*N*-acetylmuramidases, lysozymes are also capable of hydrolysing chitin, the 1,4-β-linked homopolymer of *N*-acetylglucosamine (GlcNAc). Fluorogenic substrates with 4-methylumbelliferyl (4-MeU) β-glycosides of chitin have been increasingly used for detection of chitinase activity (O'Brien & Colwell, 1987; Hood, 1991). Only the hydrolytic reaction at the aryl glycosidic bond between the GlcNAc residue and the 4-MeU group is measured fluorimetrically, which makes these substrates easy to use in kinetic measurements.

Two types of lysozymes, designated I and II, were isolated from the rainbow trout (*Oncorhynchus mykiss*) kidney (Grinde, Jollés *et al.*, 1988) and the amino-acid sequences (Dautigny *et al.*, 1991) and crystal structure (Karlsen *et al.*, 1995) showed that they belong to the c-type family. It is well known that the active site of c-type lysozymes can accommodate six sugar units (*A*–*F*; Phillips, 1966, 1967). Structural studies with RBTL and a variety of oligosaccharides have been carried out (Karlsen & Hough, 1995, 1996; Karlsen *et al.*, 1996) in order to obtain more information about the catalytic mechanism, but only nonproductive binding modes in sites *A*–*D* of the active-site cleft have been observed. The results from these studies question whether a distorted sugar conformation in site *D* is necessary for effective catalysis, as has been proposed by Blake *et al.* (1967).

The ability of lysozymes to lyse bacteria has made them commercially interesting as target enzymes in transgenic strategies directed towards improving the immune defence of

species which are used in aquaculture. The lysozymes from rainbow trout (RBTL) are particularly interesting for these kinds of experiments as they show higher activity than hen egg-white lysozyme (HEWL) against *Micrococuss luteus* and a variety of pathogenic bacteria causing problems in the aquaculture of salmon (Grinde, Lie *et al.*, 1988; Grinde, 1989*a*,*b*). Furthermore, enzyme-kinetics studies have shown that RBTL has higher catalytic activity below 293 K than HEWL, which is appropiate to cold-adapted fish species (Grinde, Jollès *et al.*, 1988).

In this paper the crystal structures of two complexes between RBTL and 4-methylumbelliferyl chitobiose [4-MeU-$(GlcNAc)_2$] and 4-methylumbelliferyl chitotriose [4-MeU-$(GlcNAc)_3$] are presented. A schematic drawing of 4-MeU-chitobiose is shown in Fig. 1. Kinetic studies on the binding of these compounds to the hen and turkey egg-white lysozymes reveal both productive (*B*–*E*) and nonproductive (*A*–*D*) binding modes (Yang & Hamaguchi, 1980), but the nonproductive binding is dominant. The equilibrium may be expressed as

$$ES_{np} \overset{K_{ES,np}}{\rightleftharpoons} E + S \overset{K_{ES,p}}{\rightleftharpoons} ES_p \overset{k_2}{\rightarrow} E + P, \qquad (1)$$

where ES_{np} and ES_p represent nonproductive ES and productive ES complexes respectively, $K_{ES,p}$ and $K_{ES,np}$ represent the binding constants for formation of the nonproductive and productive complexes, respectively, and k_2 is the rate constant for the rate-limiting step. The binding constants, K_{ES}, for 4-MeU-chitobiose and 4-MeU-chitotriose are determined to be 1.5×10^4 and $5.0 \times 10^5\ M^{-1}$, respectively, at 298 K and pH 5.18 (Yang & Hamaguchi, 1980). K_{ES} is given by $K_{ES} = K_{ES,p} + K_{ES,np}$.

2. Materials and methods

2.1. Formation of complexes, data collection and processing

Native RBTL crystals, grown as previously described (Karlsen *et al.*, 1995), were soaked with 6.5 m*M* 4-MeU-$(GlcNAc)_3$ for approximately 1 d. The complex between RBTL and 4-MeU-$(GlcNAc)_2$ was produced by co-crystallization, using the same crystallization conditions as for the native lysozyme and a 4-MeU-$(GlcNAc)_2$ concentration of 5 mg ml^{-1}. The two oligosaccharides were purchased from Sigma and the protein purified and kindly supplied by B. Grinde (Grinde, Jollès *et al.*, 1988).

Intensity data from the trigonal crystals of the two complexes were measured on a FAST area detector at room temperature using a rotating anode (40 kV, 70 mA) and Cu $K\alpha$ radiation. The two data sets were collected using two goniometer settings with a rotation of 65° in ω for each scan. Reflections were measured with a crystal-to-detector distance of 60 mm and with a width of 0.1° for each rotation image. The program *MADNES* (Pflugrath, 1989) was used during data collection and processing, and the reflections were profile-fitted in the program *XDS* (Kabsch, 1988). Merging to unique data sets was carried out using programs in the *CCP*4 program package (Collaborative Computational Project, Number 4, 1994). A summary of results from the data collections is given in Table 1.

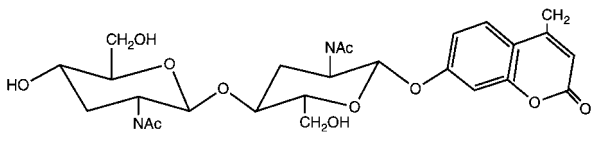

Figure 1
Chemical formula for 4-MeU-chitobiose.

Table 1
Statistics for the final data sets and refinement.

	RBTL–4-MeU-$(GlcNAc)_2$	RBTL–4-MeU-$(GlcNAc)_3$
Space group	$P3_121$	$P3_121$
Cell dimensions (Å)	$a = b = 76.42$, $c = 54.19$	$a = b = 76.69$, $c = 54.71$
Number of observations		
22.0–2.0 Å†	27802	20088
$I/\sigma(I)$ (22.0–2.0 Å)†	16.7	5.9
$I/\sigma(I)$ (2.1–2.0 Å)	7.8	1.8
Total number of unique reflections (22.0–2.0 Å)†	11498	11445
Completeness (%)		
22.0–2.0 Å†	91.8	89.5
2.2–2.1 Å	85.8	91.5
2.1–2.0 Å	83.8	42.7
Multiplicity (22.0–2.0 Å)†	2.4	1.8
R_{merge} (I) (22.0–2.0 Å)† (%)	3.4	10.5
Refinement		
Resolution (Å)	8.0–2.0	8.0–2.0
R value‡ (%)	17.5	21.1
R_{free} value§ (%)	24.3	27.1
Number of atoms	1172	1196
Protein atoms	999	999
Water molecules	132	142
Ligand atoms	41	55
R.m.s deviations from ideal geometry¶		
Bond distance (Å)	0.014	0.015
Angle distance (Å)	0.037	0.040
Planar 1–4 distance (Å)	0.042	0.038
Planarity (Å)	0.009	0.009
Average B values (Å^2)		
All atoms	21.0	18.9
All protein atoms	17.6	15.2
Main-chain atoms	16.5	14.7
Side-chain atoms	18.7	15.7
Water molecules	43.7	36.7
Ligand molecules	30.2	39.5

† Resolution for the RBTL–4-MeU-$(GlcNAc)_3$ complex: 28.0–2.0 Å. ‡ Crystallographic R factor = $\sum ||F_o| - |F_c|| / \sum |F_o|$. § R factor based on 5% randomly chosen reflections. ¶ Values from the program *PROLSQ* in the *CCP4* package (Collaborative Computational Project, Number 4, 1994).

2.2. Structure determination

The structures of the complexes were solved by difference Fourier methods using phases calculated from the 1.8 Å native RBTL structure (Karlsen *et al.*, 1995). All solvent molecules in the active-site region that were expected to interact with the substrate analogues were omitted before least-squares refinements were performed using *PROLSQ* (Hendrickson, 1985) in the *CCP*4 program package (Collaborative Compu-

tational Project, Number 4, 1994). Difference Fourier maps, $|F_{obs}(complex) - F_{calc}(native)|$, were calculated using the *CCP*4 program suite and models of the oligosaccharides were fitted to the electron density using the program *O* (Jones & Kjeldgaard, 1993). The molecular templates for generating initial coordinates of the saccharides and for setting the restraints dictionary were constructed using the program *MacroModel* (Mohamadi *et al.*, 1990) and energy minimized using the AMBER force field with a Polak–Ribiere conjugated gradient. The models of the complexes were improved during the positional refinements by inspection and manual adjustment on the graphics screen. Omit maps were calculated for uncertain parts of the substrate molecules. Initially, the individual *B* values were restrained to 20.0 Å^2 and were refined only in the last cycles of refinement. The final *R* factors are 17.5 and 21.1% for RBTL–4-MeU-$(GlcNAc)_2$ and RBTL–4-MeU-$(GlcNAc)_3$, respectively. A summary of the final refinement statistics for the two complexes is given in Table 1.

The *PEAKMAX* subroutine in the *CCP*4 suite was useful for defining peaks in the difference maps (3σ cut-off) and for locating water molecules. A water molecule was accepted if the identified peak correlated with a separate peak in the corresponding $2|F_o| - |F_c|$ map, if one or more hydrogen bonds could be formed to atoms already present in the structure and if it was not too close (less than 2.3 Å) to any other atom.

The atomic coordinates and structure factors of the two complexes have been deposited with the Protein Data Bank.

3. Results and discussion

3.1. Quality of the structures

Ramachandran plots of the refined complexes between RBTL and 4-MeU-$(GlcNAc)_2$ and 4-MeU-$(GlcNAc)_3$ generated by the program *PROCHECK* (Laskowski *et al.*, 1993) show that 91.1 and 89.3% of the residues, respectively, excluding glycines and prolines, are in the most energetically favoured regions. The remaining residues, found in additional allowed areas, are all located in flexible loops on the surface of the protein. For the complexes with 4-MeU-$(GlcNAc)_2$ and 4-MeU-$(GlcNAc)_3$, only ten and seven amino acids, respectively, have χ_1 and χ_2 side-chain torsional angles deviating more than 2.5 standard deviations from ideal geometry. Three of these side chains (Asn46, Asp101 and Asn103) are involved in the hydrogen-bonding network between the lysozyme and the bound sugar ligand.

The mean error in atomic position was estimated using the method of Luzzati (1952) and is 0.20–0.25 Å for RBTL–4-MeU-$(GlcNAc)_2$ and 0.25–0.30 Å at high resolution for RBTL–4-MeU-$(GlcNAc)_3$.

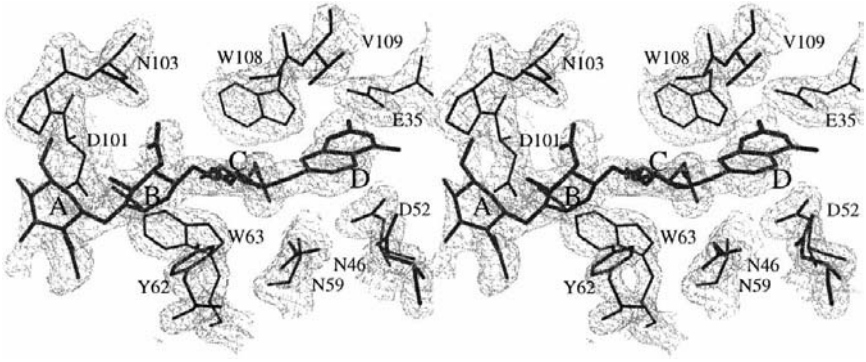

Figure 2
Electron-density map ($2|F_o| - |F_c|$, 1σ level) showing the final refined model of 4-MeU-$(GlcNAc)_3$ in subsites *A*–*D* of the active-site cleft of RBTL. The protein is marked with thin lines and the oligosaccharide with thicker lines. The figure was generated using *BOBSCRIPT* (Esnouf, 1997).

Figure 3
Ribbon drawing (*BOBSCRIPT*; Esnouf, 1997) of RBTL with 4-MeU-$(GlcNAc)_3$ bound in the active-site cleft. The ligand is represented by a ball-and-stick model.

3.2. Binding of ligands to RBTL

As is the case at native and previously solved structures of oligosaccharide complexes of RBTL (Karlsen & Hough, 1995, 1996; Karlsen *et al.*, 1995, 1996), the most poorly defined residues in the present complexes are lysine, arginine, glutamine and aspargine side chains which lie on the surface of the protein molecule. In the active-site cleft of the lysozyme, well defined electron density is found for all residues that interact with the two oligosaccharides.

Final difference ($2|F_o| - |F_c|$) maps based on the refined structures of the complexes clearly show electron density for the 4-MeU-$(GlcNAc)_2$ and 4-MeU-$(GlcNAc)_3$ molecules bound in subsites *B*–*D* and *A*–*D* of the active-site cleft of RBTL, respectively [4-MeU-$(GlcNAc)_3$ is shown in Fig. 2]. In Fig. 3 a ribbon and ball-and-stick presentation of the RBTL–4-MeU-$(GlcNAc)_3$ complex can be seen. The oligosaccharides bind to the cleft in an extended conformation with the pyranose rings in chair conformations. The sugar ring in site *A*,

however, shows some deviation from the ideal chair conformation, probably due to diffuse electron density and distortion caused in the refinement process. The torsion angles, φ and ψ, for the bound 4-MeU-chitotriose ligand about the glycosidic *A*–*B* linkage are −70 and −109°, respectively, and −73 and −112°, respectively, about the *B*–*C* linkage. φ and ψ are the torsion angles about C(1)—O(4′) and O(4′)—C(4′) defined by O(5)—C(1)—O(4′)—C(4′) and C(1)—O(4′)—C(4′)—C(5′), respectively (Mo & Jensen, 1978). As the observed φ range is −71 to −96° and the ψ range is −127 to −164° for undistorted linear polysaccharides (Jeffrey, 1990), the only value within this range is the φ angle between subsites *B* and *C*. The φ angle (−80°) between the two GlcNAc units in sites *B*–*C* in 4-MeU-chitobiose also falls within the observed φ range, but the ψ value (−115°) is lower than observed for extended oligosaccharides (Jeffrey, 1990).

For both complexes the 4-methyl-umbelliferyl moiety is bound in subsite *D*, but, as shown in Fig. 2, the electron density is slightly diffuse. It was necessary to rotate the 4-MeU-moiety about 180° from the energy-minimized model which was used as a starting template. The *N*-acetylglucosamine rings of 4-MeU-chitobiose and 4-MeU-chitotriose are bound as seen previously for the complexes between RBTL and chitin oligosaccharides (Karlsen & Hough, 1995). 4-MeU-$(GlcNAc)_2$ is bound in subsites *B* –*D* and not in *A*–*C* as seen for chitotriose bound to the hen egg-white (Cheetham *et al.*, 1992), turkey egg-white (Harata & Muraki, 1997) and partridge egg-white (Turner & Howell, 1995) lysozymes. Thus, in RBTL, sites *B*–*C* are preferred as binding sites over sites *A*–*B*.

No electron density was observed in subsite *E*, thus indicating a nonproductive binding mode for the 4-methyl-umbelliferone glycosides of the *N*-acetyl-glucosamine oligosaccharides. This observation is consistent with kinetic studies, which showed that 4-MeU-$(GlcNAc)_2$ and 4-MeU-$(GlcNAc)_3$ bind mainly in nonproductive modes to sites *B*–*D* and *A*–*D*, respectively (Yang & Hamaguchi, 1980).

A comparison of the native RBTL structure with the complexes shows that seven and ten water molecules are displaced upon binding of 4-MeU-$(GlcNAc)_2$ and 4-MeU-$(GlcNAc)_3$ to RBTL, respectively.

3.3. RBTL–ligand interactions

Detailed views of hydrogen-bonding interactions between the rainbow trout lysozyme, bound water molecules and the two 4-methylumbelliferyl chito-oligosaccharides are shown in Figs. 4(*a*) and 4(*b*). For the 4-MeU-$(GlcNAc)_3$ complex, the *N*-acetyl-glucosamine ring bound to site *A* lies almost on the surface of the active-site cleft and has only one hydrogen-bonded interaction with the protein (oxygen in the acetamido group and Asp101 OD2), but shows interactions with three water molecules (259, 261 and 273).

In both complexes the solvent-exposed *N*-acetyl side chain of the sugar moiety in subsite *B* is hydrogen bonded to the ND2 atom of Asn103 (Figs. 4*a* and 4*b*). The second hydrogen bond to the protein in this site is observed between the O atom in the hydroxymethyl group in the pyranose ring and Asp101 OD2. The other major binding interaction for site *B* is the extensive non-polar contact between the apolar face of the GlcNAc ring and the side chain of Tyr62. It has been suggested that such van der Waals contacts are characteristic of many sugar-binding proteins and are a source of substrate selectivity (Quiocho, 1986). The planes of these two rings are almost parallel and are separated by approximately 4 Å. This large hydrophobic stacking interaction, in addition to the extra hydrogen bond between the sugar and the protein in site *B* compared with site *A*, may explain why the binding energy seems to be higher for site *B* (see review by Imoto *et al.*, 1972). The GlcNAc ring in site *B* is also hydrogen bonded to three water molecules (149, 151 and 261) in the complex with 4-MeU-$(GlcNAc)_3$ and three (147, 148 and 246) in the complex with 4-MeU-$(GlcNAc)_2$.

Previously solved crystal structures of complexes between various saccharides and lysozymes have shown site *C* to be the most preferred binding site (Karlsen & Hough, 1995; Strynadka & James, 1991; Cheetham *et al.*, 1992). There are more hydrogen-bonded sugar–protein interactions, particularly for the buried 2-acetamido group, in this site than in the other sites. The binding mode of the GlcNAc ring in site *C* of 4-MeU-$(GlcNAc)_2$ and 4-MeU-$(GlcNAc)_3$ is similar to that observed previously in other lysozyme–oligosaccharide complexes. The buried 2-acetamido group interacts with the main-chain CO group of Ala107 and Asn59 NH. For both complexes, the NE1 in the plane of

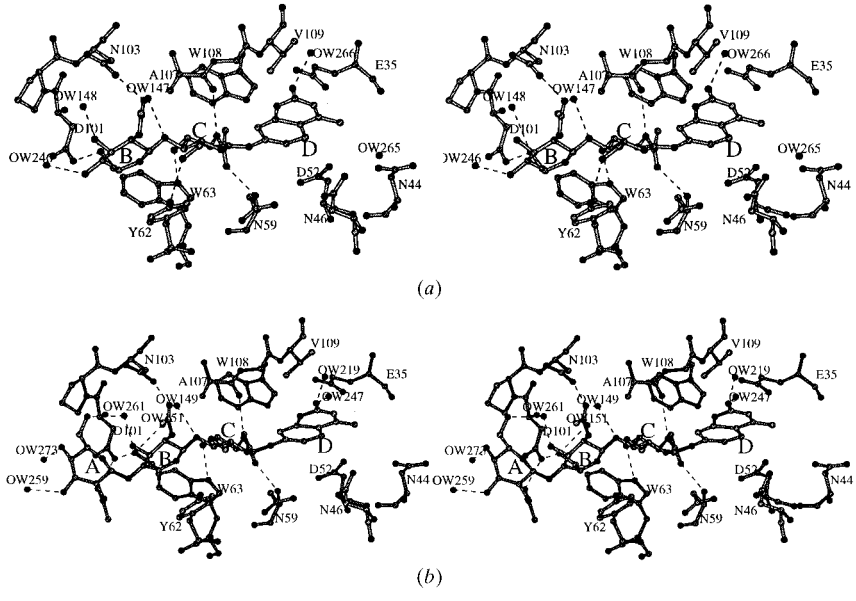

Figure 4
Hydrogen-bonding interactions between (*a*) 4-MeU-$(GlcNAc)_2$ and (*b*) 4-MeU-$(GlcNAc)_3$ and RBTL. The complexes are illustrated with ball-and-stick models and the hydrogen bonds are shown by dotted lines. The figures were generated by using the program *BOBSCRIPT* (Esnouf, 1997).

the tryptophan ring of residue 63 is orientated perpendicular to the polar face of the GlcNAc ring and makes a hydrogen bond with a exocyclic O atom of the sugar. The O atom in the hydroxymethyl group of the pyranose ring is hydrogen bonded to the the hydroxyl group of Tyr62 in the complex between RBTL and 4-MeU-$(GlcNAc)_2$, a contact that may position the tyrosine ring in the correct orientation for interactions with the pyranose ring in site *B*.

The observations that $(GlcNAc)_2$, $(GlcNAc)_3$ (Karlsen & Hough, 1995) and 4-MeU-$(GlcNAc)_2$ bind in subsites *B*–*D* of RBTL and not in *A*–*C*, as observed for the hen, partridge and turkey egg-white lysozymes (Cheetham *et al.*, 1992; Turner & Howell, 1995; Harata & Muraki, 1997), could be explained from the fact that residue 62 is a tyrosine in RBTL and not a tryptophan as in the other mentioned lysozymes. It is possible that in RBTL the tyrosine ring, which is smaller than the tryptophan, makes less extensive van der Waals contacts with the sugar ring in the *B* site. One consequence might be that the pyranose ring is more weakly bound in site *B* of RBTL than in the other c-type lysozymes, and the oligosaccharides might be forced into site *C*, which is, as mentioned above, a much better binding site than site *A*.

In both complexes, the 4-MeU ring bound in site *D* is not hydrogen bonded to the protein but shows interactions with water molecules. In the RBTL–4-MeU-$(GlcNAc)_3$ complex, the exocyclic O atom is bound to waters 219 and 247 (see Fig. 4*b*), and in the RBTL–4-MeU-$(GlcNAc)_2$ complex, hydrogen bonds are seen to water 266 (see Fig. 4*a*). For both complexes, no hydrogen bonds are seen to Glu35 and Asp52, which are supposed to play an important function in the catalytic mechanism (Blake *et al.*, 1967). This is not surprising, taking into consideration the observation that the 4-MeU ring is flat and not puckered like the GlcNAc unit in the natural lysozyme substrate.

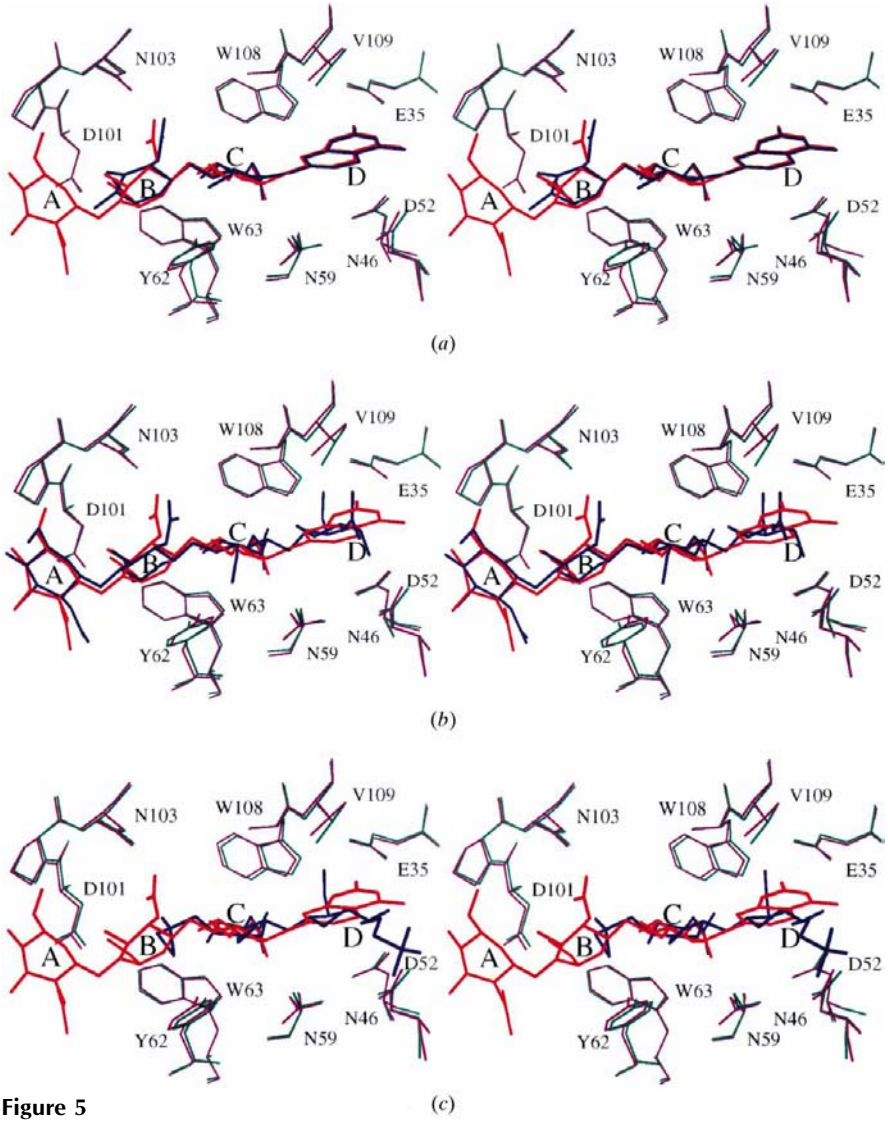

Figure 5
All figures were generated using *BOBSCRIPT* (Esnouf, 1997). (*a*) A superimposition of 4-MeU-$(GlcNAc)_2$ (blue) on 4-MeU-$(GlcNAc)_3$ (red) in the active-site cleft of RBTL. The protein models in the former and latter complexes are coloured green and purple, respectively. (*b*) A superimposition of RBTL–4-MeU-$(GlcNAc)_3$ (purple/red) and RBTL–$(GlcNAc)_4$ (green/blue) (Karlsen & Hough, 1995). (*c*) A superimposition of RBTL–4-MeU-$(GlcNAc)_3$ (purple/red) and RBTL–bulgecin (green/blue) (Karlsen & Hough, 1996).

3.4. Comparison of binding modes

A superimposition of the complexes between RBTL and 4-MeU-$(GlcNAc)_2$ and 4-MeU-$(GlcNAc)_3$ (Fig. 5*a*) shows that the oligosaccharides bind in the same way to the active-site cleft. The binding mode of the saccharide in subsite *B* is somewhat different, which may be a consequence of the lack of binding of a saccharide to site *A* for 4-MeU-$(GlcNAc)_2$. Fig. 5(*a*) also shows that the residues in the active-site cleft which interact with the sugars have similar conformations in the two complexes.

The binding modes of 4-MeU-chitotriose and chito-tetraose (Karlsen & Hough, 1995) were also compared (Fig. 5*b*) and are found to be very similar. As the 4-MeU ring is planar while the GlcNAc unit has a chair conformation, the binding modes and interactions in subsite *D* are different. The bacterial metabolite bulgecin, shown in Fig. 6, binds to subsites *C* and *D* in a similar way to 4-MeU-$(GlcNAc)_3$ (Fig. 5*c*), with its proline ring bound to site *D*. The taurine moiety of bulgecin binds to the left side of the active cleft of RBTL, where it interacts with Asn46 and Thr47 (Karlsen & Hough, 1996).

3.5. The flexibility of the complexes

As seen in Table 1, the average temperature factors for RBTL–4-MeU-

Table 2
Average temperature factors for 4-MeU-$(GlcNAc)_2$ and 4-MeU-$(GlcNAc)_3$ bound in the active-site cleft of RBTL.

Binding site	4-MeU-$(GlcNAc)_2$ $B_{average}$ (Å^2)	4-MeU-$(GlcNAc)_3$ $B_{average}$ (Å^2)
A	—	42.8
B	25.3	37.1
C	24.2	35.7
D	41.8	42.6

$(GlcNAc)_2$ and RBTL–4-MeU-$(GlcNAc)_3$ are 16.5 and 14.7 Å^2 for main-chain and 18.7 and 15.7 Å^2 for side-chain atoms, respectively. The corresponding values for the native enzyme are 22.0 and 26.9 Å^2 (Karlsen *et al.*, 1995), indicating that the complexes are less flexible than the native structure. This trend can also be seen in Fig. 7, where the average temperature factors for the main-chain atoms are plotted as a function of the residue number of the two complexes and the native RBTL. As data for the native structure were collected on an R-AXIS image plate (Karlsen *et al.*, 1995) and data for the complexes on a FAST system (both at room temperature), differences in flexibility might be due to differences in the data.

The temperature-factor plot shows that in common with the native structure, the areas that exhibit the highest flexibility are found in the external loops from residues 45–50, which form a β-bend in the three-stranded β-sheet area, residues 62–75, in a long coiled loop, and residues towards the C terminus. These loops also show the greatest deviation between the native and complexed RBTL structures. The r.m.s. deviations between native RBTL and RBTL complexed with 4-MeU-$(GlcNAc)_2$ and 4-MeU-$(GlcNAc)_3$ are 0.42 and 0.67 Å for all atoms, respectively, showing that the latter complex deviates most from the native structure. The region with the most striking differences in main-chain position is the loop consisting of residues 70–75, which is located on the surface of the protein. This loop becomes less flexible and shifts towards the active site where it anchors Trp62, which interacts with the saccharide unit in subsite C. The interactions between Asn44 and Asn46 in RBTL and the oligosaccharides also make the residue 44–50 loop less flexible in the complexes.

Table 1 shows that the average temperature factors for 4-MeU-$(GlcNAc)_2$ and 4-MeU-$(GlcNAc)_3$ are 30.2 and 39.5 Å^2, respectively, indicating that the latter oligosaccharide is more loosely bound than the former. The differences in the *B* factors could be due to differences in occupancies. As the complexes between RBTL and 4-MeU-$(GlcNAc)_2$ and between RBTL and 4-MeU-$(GlcNAc)_3$ were made by co-crystallization and soaking, respectively, it seems reasonable that the occupancy of the saccharide in the latter complex might be lower than for the former complex. Table 2, which gives a survey of the average temperature factors for the two oligosaccharides bound to the active-site cleft, shows that the sugar in site *A* is most loosely bound to the protein. As previously observed in oligosaccharide–lysozyme complexes (Karlsen & Hough, 1995), site *C* is the most specific and preferred binding site, but subsite *D* seems to be quite flexible. This is not surprising, as earlier observations have shown that the 4-MeU moiety is only bound to water molecules and not to protein atoms which can stabilize the enzyme–substrate complex.

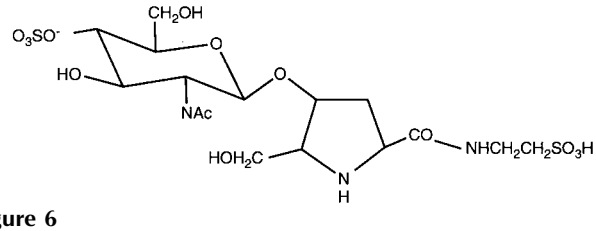

Figure 6
Chemical formula for bulgecin.

4. Concluding remarks

It has been well known for a long time that lysozymes cleave the glycosidic bond between saccharides bound to subsites *D* and *E* in the active-site cleft (Blake *et al.*, 1967). The 4-methylumbelliferyl glycosides of chitin are used as substrates in lysozyme assays (O'Brien & Colwell, 1987; Hood, 1991), indicating that the glycosidic bond between GlcNAc and 4-MeU is broken. Based on these facts, one might expect the 4-methylumbelliferone glycosides of *N*-acetylglucosamine to bind with the 4-methylumbelliferyl part in site *E*.

The results from the crystallographic studies of the complexes between RBTL and 4-MeU chitobiose and chitotriose clearly show electron density in sites *B*–*D* and *A*–*D*, respectively. Thus, the saccharides have the same nonproductive binding mode as previously observed for complexes between RBTL and oligosaccharides of chitin (Karlsen & Hough, 1995). Our crystallographic results confirm the results from kinetic studies by Yang & Hamaguchi (1980), showing that 4-MeU-$(GlcNAc)_2$ and 4-MeU-$(GlcNAc)_3$ bind mainly to

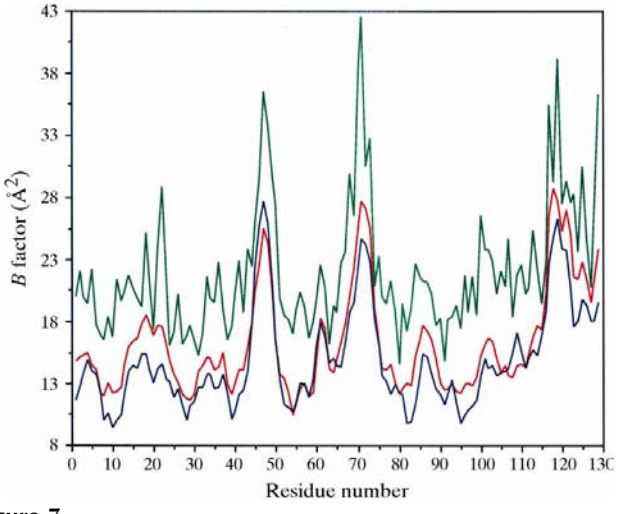

Figure 7
Variation in isotropic temperature factors *B* (Å^2) averaged over main-chain atoms along the polypeptide chain for native RBTL (green line) and RBTL in complex with 4-MeU-$(GlcNAc)_2$ (red line) and with 4-MeU-$(GlcNAc)_3$ (blue line).

subsites *B*–*D* and A–*D*, respectively. Thus, the equilibrium in equation (1) lies far to the left, towards the nonproductive ES_{np} complex. Time-resolved experiments at low temperature will hopefully make it possible to 'catch' the productive ES complex before dissociation.

This work was supported by the Norwegian Research Council. We would like to thank Dr B. Grinde for supplying us with the purified rainbow trout lysozyme and Cand. Scient. M. Skar for model building and energy minimization of 4-MeU-chitotriose.

References

Blake, C. C. F., Johnson, L. N., Mair, G. A., North, A. C. T., Phillips, D. C. & Sarma, V. R. (1967). *Proc. R. Soc. London Ser. B*, **167**, 378–388.
Cheetham, J. C., Artymiuk, P. J. & Phillips, D. C. (1992). *J. Mol. Biol.* **224**, 613–628.
Collaborative Computational Project, Number 4 (1994). *Acta Cryst.* D**50**, 760–763.
Dautigny, A., Prager, E. M., Pham-Dinh, D., Jollés, J., Pakdel, F., Grinde, B. & Jollés, P. (1991). *J. Mol. Evol.* **32**, 187–198.
Esnouf, R. M. (1997). *J. Mol. Graph.* **15**, 133–138.
Grinde, B. (1989*a*). *J. Fish Dis.* **12**, 95–104.
Grinde, B. (1989*b*). *FEMS Micobiol. Lett.* **60**, 179–182.
Grinde, B., Jollés, J. & Jollés, P. (1988). *Eur. J. Biochem.* **173**, 269–273.
Grinde, B., Lie, Ø., Poppe, T. & Salte, R. (1988). *Aquaculture*, **68**, 299–304.
Harata, K. & Muraki, M. (1997). *Acta Cryst.* D**53**, 650–657.
Hendrickson, W. A. (1985). *Methods Enzymol.* **115**, 252–270.
Hood, M. A. (1991). *J. Microbiol. Methods*, **13**, 151–160.
Imoto, T., Johnson, L. N., North, A. C. T., Phillips, D. C. & Rupley, J. A. (1972). *The Enzymes*, Vol. VII, *Vertebrate Lysozymes*, pp. 665–868. New York & London: Academic Press.
Jeffrey, G. A. (1990). *Acta Cryst.* B**46**, 89–103.
Jones, T. A. & Kjeldgaard, M. (1993). *O – The Manual*, version 5.9.1. Uppsala, Sweden.
Kabsch, W. (1988). *J. Appl. Cryst.* **21**, 67–71.
Karlsen, S., Eliassen, B. E., Hansen, L. K., Larsen, R. L., Riize, B. W., Smalås, A. O., Hough, E. & Grinde, B. (1995). *Acta Cryst.* D**51**, 354–367.
Karlsen, S. & Hough, E. (1995). *Acta Cryst.* D**51**, 962–978.
Karlsen, S. & Hough, E. (1996). *Acta Cryst.* D**52**, 115–123.
Karlsen, S., Hough, E., Rao, Z. H. & Isaacs, N. W. (1996). *Acta Cryst.* D**52**, 105–114.
Laskowski, R. A., MacArthur, M. W., Moss, D. S. & Thornton, R. M. (1993). *J. Appl. Cryst.* **26**, 283–291.
Luzzati, P. V. (1952). *Acta Cryst.* **5**, 802–810.
Mo, F. & Jensen, L. H. (1978). *Acta Cryst.* B**34**, 1562–1569.
Mohamadi, F., Richards, N. G. J., Guida, W. C., Liskamp, R., Lipton, M., Caufield, C., Chang, G., Hendrickson, T. & Still, W. C. (1990). *J. Comput. Chem.* **11**, 440–467.
O'Brien, M. & Colwell, R. R. (1987). *Appl. Environ. Microbiol.* **53**, 1718–1720.
Pflugrath, J. W. (1989). *MADNES*, *Munich Area Detector NE System User's Guide*. Cold Spring Harbor Laboratory Press.
Phillips, D. C. (1966). *Sci. Am.* **215**, 78–90.
Phillips, D. C. (1967). *Proc. Natl Acad. Sci. USA*, **57**, 484–495.
Quiocho, F. A. (1986). *Annu. Rev. Biochem.* **55**, 287–315.
Strynadka, N. C. J. & James, M. N. G. (1991). *J. Mol. Biol.* **220**, 401–424.
Turner, M. A. & Howell, P. L. (1995). *Protein Sci.* **4**, 442–449.
Yang, Y. & Hamaguchi, K. (1980). *J. Biochem.* **87**, 1003–1014.